

# Exactly Robust Kernel Principal Component Analysis

Jicong Fan, Tommy W.S. Chow

**Abstract**—We propose a novel method called robust kernel principal component analysis (RKPCA) to decompose a partially corrupted matrix as a sparse matrix plus a high or full-rank matrix whose columns are drawn from a nonlinear low-dimensional latent variable model. RKPCA can be applied to many problems such as noise removal and subspace clustering and is so far the only unsupervised nonlinear method robust to sparse noises. We also provide theoretical guarantees for RKPCA. The optimization of RKPCA is challenging because it involves nonconvex and indifferentiable problems simultaneously. We propose two nonconvex optimization algorithms for RKPCA: alternating direction method of multipliers with backtracking line search and proximal linearized minimization with adaptive step size. Comparative studies on synthetic data and nature images corroborate the effectiveness and superiority of RKPCA in noise removal and robust subspace clustering.

**Index Terms**—RPCA, low-rank, high-rank, kernel, sparse, noise removal, subspace clustering.

## I. INTRODUCTION

**P**RINCIPAL component analysis (PCA) [1] is a well-known and powerful technique that has been widely used in many areas such as computer science, economy, biology, and chemistry. In these areas, the data are often redundant and can be represented by a few number of features. The basic idea of PCA is to find a set of orthogonal projections to transform the high-dimensional data or observed variables into low-dimensional latent variables while the reconstruction errors are minimized. The orthogonal projections can be found by singular value decomposition or eigenvalue decomposition. PCA can be used for dimensionality reduction, feature extraction, and noise removal.

PCA is a linear method that is not effective in handling nonlinear data. To solve the problem, kernel PCA (KPCA) [2] was proposed. In KPCA, the observed data are transformed by a nonlinear function into a high (possibly infinite) dimensional feature space; by using kernel trick, the latent variables can be extracted from the feature space without explicitly carrying out the nonlinear mapping. KPCA has been applied to solve many practical problems such as dimensionality reduction, novelty detection [3], [4], and image denoising [5]. It is worth noting that KPCA cannot be directly applied to denoising problems. In [5]–[7], the pre-image problem of KPCA was studied. In the problem, the principal components obtained from the feature space are mapped back to the data space to reconstruct

The authors are with the Department of Electronic Engineering, City University of Hong Kong, Kowloon, Hong Kong SAR, China.  
Corresponding author: Jicong Fan. E-mail: jicongfan2-c@my.cityu.edu.hk

the observed variables, where the reconstruction errors are regarded as the noises. In [8], a robust KPCA was proposed to treat noise, missing data, and outliers in KPCA.

Another limitation of PCA is that it is not robust to sparse corruptions and outliers. To solve problem, a few robust methods were proposed for PCA [9]–[11]. In [11], RPCA decomposes a noisy matrix into a low-rank matrix plus a sparse matrix, which are obtained through rank minimization and soft thresholding. RPCA can be solved by inexact augmented Lagrange multiplier method or alternating direction method of multipliers [12]. The low-rank or/and sparse models have been widely studied and exploited in many problems such as matrix completion [13]–[15] and robust subspace clustering [16]–[18]. In robust subspace clustering, RPCA could outperform the low-rank representation (LRR) and sparse representation (SSC) based subspace clustering methods when the data are heavily corrupted by sparse noises or/and outliers. The reason is that the dictionary used in LRR and SSC is the data matrix itself and hence introduces considerable bias for the representations. A few recent extensions of RPCA can be found in [19]–[22].

It should be pointed out that KPCA is not robust to sparse noises and RPCA is unable to handle nonlinear data and high-rank matrices. Therefore, it is quite necessary to propose a variant of PCA that is not only able to handle nonlinear data but also robust to sparse noises. It is worth noting that the robust KPCA proposed in [8] is a supervised method for handling sparse noises and outliers. It requires the training data have no sparse noises and outliers. Otherwise, the method is similar to the KPCA pre-image methods proposed in [5], [6].

In this paper, we propose a novel method called robust kernel principal component analysis (RKPCA) to handle nonlinear data and sparse noises simultaneously. RKPCA assumes that the nonlinear transformation of the data matrix is of low-rank while RPCA assumes that the data matrix itself is of low-rank. RKPCA is effective in recovering high-rank or even full-rank matrices and robust to sparse noises and outliers. We also provide theoretical support for RKPCA. The optimization of RKPCA is challenging because nonconvex and indifferentiable problems simultaneously exist. We propose nonconvex alternating direction method of multipliers with backtracking line search and nonconvex proximal linearized minimization with adaptive step size for RKPCA. Comparative studies are conducted on synthetic data and nature images. The experimental results verify that: (1) RKPCA is more effective than PCA, KPCA, and RPCA in recognizing sparse noises

when the data have nonlinear structures; (2) RKPCA is more robust and effective than RPCA, SSC, and LRR in subspace clustering.

## II. METHODOLOGY

### A. Theory and model of RKPCA

Assume that a  $d \times n$  observed data matrix  $M$  is given by

$$M = X + E, \quad (1)$$

where  $X$  is the matrix of clean data and  $E$  is the matrix of sparse noises (randomly distributed), our goal is to recover  $X$  and  $E$ . In RPCA,  $X$  is assumed to be of low-rank. Hence, RPCA aims at solving the following problem

$$\min_{X, E} \text{rank}(X) + \lambda \|E\|_0, \text{ s.t. } X + E = M, \quad (2)$$

where  $\text{rank}(X)$  denotes the rank of  $X$ ,  $\|E\|_0$  is the  $\ell_0$  norm of  $E$  defined by the number of non-zero elements in  $E$ , and  $\lambda$  is a parameter to balance the two terms. Both rank minimization and  $\ell_0$  norm minimization are NP-hard. Therefore, problem (2) is approximated as

$$\min_{X, E} \|X\|_* + \lambda \|E\|_1, \text{ s.t. } X + E = M, \quad (3)$$

where  $\|X\|_*$  denotes the nuclear norm of  $X$  and  $\|E\|_1$  denotes the  $\ell_1$  norm of  $E$ . Nuclear norm, defined by the sum of singular values, is a convex relaxation of matrix rank.  $\ell_1$  norm is a convex relaxation of  $\ell_0$  norm. Nuclear norm minimization and  $\ell_1$  norm minimization can be solved by singular value thresholding and soft thresholding respectively.

The low-rank assumption made in RPCA indicates that  $X$  is from a low-dimensional linear latent variable model, i.e.,  $X = PZ$ , where  $P \in \mathbb{R}^{d \times r}$  is the projection matrix,  $Z \in \mathbb{R}^{r \times n}$  consists of the latent variables, and  $r$  is the rank of  $X$ . In practice, many data are drawn from low-dimensional nonlinear latent variable models, e.g.,

$$X = f(Z), \quad (4)$$

where  $f(\cdot) : \mathbb{R}^r \rightarrow \mathbb{R}^d$  is a nonlinear function that performs on each column of  $Z \in \mathbb{R}^{r \times n}$  separately. Although  $r$  is much smaller than  $d$ ,  $X$  could be of high-rank or even full-rank, which is beyond the assumption of RPCA. Therefore  $X$  and  $E$  cannot be recovered by RPCA. We denote the latent or intrinsic dimensionality of  $X$  by  $ldim(X)$  and have  $ldim(X) \leq \text{rank}(X)$ , where the equality holds when  $f(\cdot)$  is linear.

To make the recovery problem meaningful, we propose the following assumption:

**Assumption 1. (non-sparse component condition)** Given  $f(\cdot) : \mathbb{R}^r \rightarrow \mathbb{R}^d$  and  $z \in \mathbb{R}^{r \times 1}$ , ones has  $f(z) = \sum_{i=1}^r f_i(z_i)$ , where  $f_{ji}(z_i) \neq 0 \forall j = 1, \dots, d$  and  $i = 1, \dots, r$ .

As  $X = \sum_{i=1}^r X_i = \sum_{i=1}^r f_i(Z_{i \cdot})$ , Assumption 1 indicates that every component  $X_i$  is not sparse. As a result, given a matrix  $X' = X - X_i$ , where  $ldim(X') = r - 1$ , we have  $E' = E + X_i$ , which is not sparse. On the contrary, if there is no Assumption 1,  $E' = E + X_i$  could be sparse, which indicates that  $X$  cannot be exactly recovered although  $E$  is sparse. In a

word, Assumption 1 ensures that the latent dimension of the optimal  $X$  is  $r$  when  $E$  is sparse. Assumption 1 is similar to the incoherence condition [11] in RPCA. However, it is difficult to further quantify Assumption 1 because  $f(\cdot)$  cannot be readily determined.

Under Assumption 1, we give the following lemma:

**Lemma 1.**  $X$  and  $E$  can be recovered through solving

$$\min_{X, E} ldim(X) + \lambda \|E\|_0, \text{ s.t. } X + E = M, \quad (5)$$

where  $r/(dn - e) < \lambda < d/e$  and  $e = \|E\|_0$ .

*Proof.* Denote the optimal value of  $X$  and  $E$  by  $X^*$  and  $E^*$ . Denote  $J(X, E) = ldim(X) + \lambda \|E\|_0$ . Then  $J(X^*, E^*) = r + \lambda e$ . Given an arbitrary  $X' = X^* + \Delta$  with  $\Delta \neq 0$ : if  $ldim(X') < r$ , with Assumption 1, we have  $J(X', E') = r' + \lambda e' > J(X^*, E^*)$ ; if  $ldim(X') > r$ , we have  $J(X', E') > r + d > J(X^*, E^*)$ ;  $J(X', E') = J(X^*, E^*)$  only if  $\Delta = 0$ .  $\square$

Though (5) is intractable, lemma 1 indicates the feasibility that  $X$  can be recovered when  $f(\cdot)$  is nonlinear. If we can find a tractable approximation or relaxation of (5) (especially for  $ldim(X)$ ), then  $X$  and  $E$  can be solved.

In this paper, we give the following assumption:

**Assumption 2.** Given  $X = f(Z)$  ( $f(\cdot) : \mathbb{R}^r \rightarrow \mathbb{R}^d, r < d$ ), there exists a nonlinear function  $\phi(\cdot)$  that maps  $X$  into a high-dimensional (possibly infinite) feature space  $\mathcal{F}^\kappa$  such that the matrix  $\Phi(X) \in \mathbb{R}^{\kappa \times n}$  is of low-rank (or approximately), where

$$\phi(\cdot) : \mathbb{R}^d \rightarrow \mathcal{F}^\kappa \quad (6)$$

and  $\Phi(X) = [\phi(x_1), \dots, \phi(x_n)]$ .

*Proof.* We denote  $\phi(x) = \phi(f(z)) = \psi(z)$ . Using Taylor series, we have

$$\Psi(z) = \sum_{|\alpha| \leq 0} \frac{(z - \bar{z})^\alpha}{\alpha!} (\partial^\alpha \phi)(\bar{z}), \quad (7)$$

where we have used the multi-index notation. The  $p$ -th order Taylor approximation of  $\Psi(z)$  can be given as

$$\Psi(z) \approx C_0 + C_1 \chi_1 + \dots + C_p \chi_p, \quad (8)$$

where  $C_0 \in \mathbb{R}^{\kappa \times 1}$ . For  $k = 1, \dots, p$ ,  $C_k \in \mathbb{R}^{\kappa \times d_k}$ ,  $\chi_k \in \mathbb{R}^{d_k \times 1}$  consists of the  $k$ -combinations (product) of the elements in  $z - \bar{z}$ , and  $d_k = \binom{r+k-1}{k}$ . Denote  $\Psi(Z) = [\psi(z_1), \psi(z_2), \dots, \psi(z_n)]$ , then we have

$$\text{rank}(\Psi(Z)) = 1 + \sum_{k=1}^p \binom{r+k-1}{k}, \quad (9)$$

provided that  $n$  and  $\kappa$  are large. It indicates that  $\Phi(X)$  is of low-rank (or approximately). For example, when  $d = 10$ ,  $r = 2$ ,  $n = 100$ , and  $p = 4$ , we have  $\text{rank}(\Phi(X)) = 15 \ll 100$ , although  $X$  could be of full-rank.  $\square$

Suppose that, when  $X$  is clean, the rank of  $\Phi(X)$  is  $r_{\Phi(X)}$ . If  $X$  is corrupted by sparse noises, e.g.,  $\hat{X} = X + \hat{E}$  and  $\hat{E} \neq 0$ , the rank of  $\Phi(\hat{X})$  will be higher than that of  $\Phi(X)$ , i.e.,

$$r_{\Phi(\hat{X})} > r_{\Phi(X)}. \quad (10)$$

Therefore, to recover  $X$  from  $M$ , we can minimize the rank of  $\Phi(X)$ . To avoid that the rank of  $\Phi(X)$  is lower than its true value  $r_{\Phi(X)}$ , we have to make sure that  $E$  is sparse. Therefore, we propose to solve the following problem

$$\min_{X,E} \text{rank}(\Phi(X)) + \lambda \|E\|_0, \text{ s.t. } X + E = M. \quad (11)$$

With (10), we can see that the solutions of (11) are exactly the true values of  $X$  and  $E$ . Problem (11) can be further approximated by

$$\min_{X,E} \|\Phi(X)\|_* + \lambda \|E\|_1, \text{ s.t. } X + E = M, \quad (12)$$

where  $\|\Phi(X)\|_* = \sum_{i=1}^{\min(\kappa,n)} \sigma_i$  and  $\sigma_i$  is the  $i$ th singular value of  $\Phi(X)$ . We also have

$$\|\Phi(X)\|_* = \text{tr}((\Phi(X)^T \Phi(X))^{1/2}), \quad (13)$$

where  $\text{tr}(\cdot)$  denotes matrix trace. Denoting the SVD of  $\Phi(X)$  by  $\Phi(X) = USV^T$ , equation (13) can be proved as following:

$$\begin{aligned} \text{tr}((\Phi(X)^T \Phi(X))^{1/2}) &= \text{tr}((VS^2V^T)^{1/2}) \\ &= \text{tr}(V(S^2)^{1/2}V^T) = \text{tr}(S) = \|\Phi(X)\|_*. \end{aligned} \quad (14)$$

Substituting (13) into problem (11), we get

$$\min_{X,E} \text{tr}((\Phi(X)^T \Phi(X))^{1/2}) + \lambda \|E\|_1, \text{ s.t. } X + E = M. \quad (15)$$

In the  $n \times n$  Gram matrix  $\Phi(X)^T \Phi(X)$ , each element  $\phi(x_i)^T \phi(x_j) = \langle \phi(x_i), \phi(x_j) \rangle$  can be directly obtained by kernel representations [2], i.e.,

$$\langle \phi(x_i), \phi(x_j) \rangle = k(x_i, x_j), \quad (16)$$

without carrying out  $\phi(\cdot)$  explicitly. In (16),  $k(\cdot, \cdot)$  is a kernel function satisfying Mercer's theorem [2]. With a certain kernel function  $k(\cdot, \cdot)$ , the nonlinear mapping  $\phi(\cdot)$  and the feature space  $\mathcal{F}$  will be implicitly determined. The most widely-used kernel function is the radial basis function (RBF) kernel

$$k(x, y) = \exp(-\|x - y\|^2/(2\sigma^2)), \quad (17)$$

where  $\sigma$  is a free parameter controlling the smoothness degree of the kernel. The dimensionality of the feature space  $\mathcal{F}$  given by RBF kernel is infinite.

With the kernel matrix  $K = [k(x_i, x_j)]_{n \times n} = [\phi(x_i)^T \phi(x_j)]_{n \times n}$ , problem (15) can be rewritten as

$$\min_{X,E} \text{tr}(K^{1/2}) + \lambda \|E\|_1, \text{ s.t. } X + E = M. \quad (18)$$

According to Lemma 1, since  $\text{tr}(K^{1/2})$  and  $\|E\|_1$  are the relaxations of  $\text{ldim}(X)$  and  $\|E\|_0$  in (5),  $X$  and  $E$  can be recovered through solving (18) for certain  $\lambda$ . We call the proposed method robust kernel PCA (RKPCA), which is able to handle nonlinear data and sparse noises simultaneously. Moreover, since the nonlinear data often form high-rank matrices, RKPCA is able to recover  $X$  and  $E$  even if  $X$  is of high-rank or full-rank. On the contrary, RPCA cannot effectively recover high-rank matrices and full-rank matrices.

The parameter  $\lambda$  is crucial to RKPCA. In (18),  $\text{tr}(K^{1/2})$  and  $\|E\|_1$  may have different orders of magnitude. When RBF kernel is used, we have

$$\sqrt{n} < \text{tr}(K^{1/2}) < n. \quad (19)$$

To balance the two terms in (18) or (12),  $\lambda$  should be determined as

$$\lambda = n\lambda_0/\|M\|_1, \quad (20)$$

where the value of  $\lambda_0$  can be chosen around 0.5.

In the following context, we will provide the theoretical guarantee of RKPCA and compare it with that of RPCA. In [11], the following theorem (reformulated) was proved for RPCA:

**Theorem 1.** *With the incoherence assumption [11], RPCA is able to exactly recover  $X$  (low-rank) and  $E$  (sparse) with high probability at least  $1 - cn^{-10}$ , provided that*

$$\text{rank}(X) \leq \rho_r \mu^{-1} n_{(2)} (\log n_{(1)})^{-2} \text{ and } m/(dn) \leq \rho_s. \quad (21)$$

Above,  $c$ ,  $\rho_r$ , and  $\rho_s$  are numerical constants;  $m$  is the number of nonzero entries of  $E$ ;  $\mu$  is the parameter of incoherence condition;  $n_{(1)} = \max(d, n)$  and  $n_{(2)} = \min(d, n)$ .

In this paper, we make the following assumptions:

**Assumption 3.** *With the non-sparse component condition in Assumption 1 and the nonlinear mapping in Assumption 2, the SVD of  $\Phi(X)$  meets the incoherence condition with parameter  $\mu$ .*

**Assumption 4.** *(a) the constraint  $X + E = M$  is implicitly transformed to  $\Phi(X) + \mathcal{E} = \mathcal{M}$  in the feature space; (b)  $\mathcal{E}$  is sparse and the number of nonzero elements is  $m = c_s \rho_s n^2$ , where  $c_s$  is a numerical constant.*

With Assumption 4, RKPCA in (12) is reformulated as

$$\min_{\Phi(X), \mathcal{E}} \|\Phi(X)\|_* + \lambda \|\mathcal{E}\|_1, \text{ s.t. } \Phi(X) + \mathcal{E} = \mathcal{M}, \quad (22)$$

which has the same format as that of RPCA. Then we give the following theorem:

**Theorem 2.** *With Assumptions 3 and 4, RKPCA is able to exactly recover  $X$  (high-rank) and  $E$  (sparse) with high probability at least  $1 - cn^{-10}$ , provided that*

$$\text{rank}(\Phi(X)) \leq \rho_r \mu^{-1} n (\log n)^{-2} \text{ and } m/n^2 \leq c_s \rho_s. \quad (23)$$

*Proof.* We can prove that RKPCA is able to recover  $\Phi(X)$  (low-rank) and  $\mathcal{E}$  (sparse) with high probability using the similar approach in RPCA [11]. Since  $\Phi(X)$  and  $\mathcal{E}$  correspond to  $X$  and  $E$ , it indicates that RKPCA can recover  $X$  and  $E$  successfully.  $\square$

More intuitively, according to Assumption 2 and formula (9), it is reasonable to represent  $\text{rank}(\Phi(X))$  as  $\text{rank}(\Phi(X)) = c_{fk} \text{ldim}(X)$ , where  $c_{fk} \geq 1$  is a constant related with the property of  $f(\cdot)$  and  $k(\cdot, \cdot)$ . Then (23) can be rewritten as

$$\text{ldim}(X) \leq \rho_r \mu^{-1} n / c_{fk} (\log n)^{-2} \text{ and } m/n^2 \leq c_s \rho_s. \quad (24)$$

Comparing (24) with (21), we make the following conclusions: (a) suppose  $d < n$ , RPCA requires  $\text{rank}(X)$  is on the order of  $d(\log n)^{-2}$  while RKPCA requires  $\text{ldim}(X)$  is on the order of  $n/c_{fk}(\log n)^{-2}$ ; (b) when  $n$  increases, the upper bound of  $\text{ldim}(X)$  also increases; (c) when

$\text{rank}(X) = d$  (full-rank), RPCA fails but RKPCA works because  $\text{ldim}(X) < \text{rank}(X) < n$ .

It is worth noting that in RKPCA the nuclear norm  $\|\Phi(X)\|_*$  is a special case (when  $p = 1$ ) of the Schatten  $p$ -norm  $\|\Phi(X)\|_{Sp}^p = \left(\sum_{i=1}^{\min(\kappa, n)} (\sigma_i)^p\right)^{1/p}$  ( $0 < p \leq 1$ ), which is a nonconvex relaxation of matrix rank. We have  $\|\Phi(X)\|_{Sp}^p = \text{tr}(K^{p/2})$  and get the Schatten  $p$ -norm based RKPCA, which has nearly the same optimization approach as that of the nuclear norm based RKPCA.

### B. Optimization for RKPCA

#### 1) ADMM plus backtracking line search (ADMM+BTLS):

In RKPCA formulated by (18), the two blocks of unknown variables  $X$  and  $E$  are separable. The second term  $\lambda\|E\|_1$  and the constraint are convex. The first term  $\text{tr}(K^{1/2})$  could be nonconvex if a nonlinear kernel such as RBF kernel is used. We propose to solve (18) via alternating direction method of multipliers (ADMM) [23]–[25]. The augmented Lagrangian function of (18) is given by

$$\begin{aligned} \mathcal{L}(X, E, Q) = & \text{tr}(K^{1/2}) + \lambda\|E\|_1 \\ & + \langle X + E - M, Q \rangle + \frac{\mu}{2}\|X + E - M\|_F^2, \end{aligned} \quad (25)$$

where  $Q \in \mathbb{R}^{d \times n}$  is the matrix of Lagrangian multipliers and  $\mu > 0$  is a penalty parameter.  $\mathcal{L}(X, E, Q)$  can be minimized over  $X$  and  $E$  one after another.

First, fix  $E$  and solve

$$\min_X \text{tr}(K^{1/2}) + \frac{\mu}{2}\|X + E - M + Q/\mu\|_F^2. \quad (26)$$

Because of the kernel matrix  $K$ , problem (26) has no closed-form solution. Denoting

$$\mathcal{J} = \text{tr}(K^{1/2}) + \frac{\mu}{2}\|X + E - M + Q/\mu\|_F^2, \quad (27)$$

we propose to solve (26) with gradient descent, i.e.,

$$X \leftarrow X - \eta \frac{\partial \mathcal{J}}{\partial X}. \quad (28)$$

where  $\eta$  is the step size and will be discussed later. Denoting  $\mathcal{J}_1 = \text{tr}(K^{1/2})$  and  $\mathcal{J}_2 = \frac{\mu}{2}\|X + E - M + Q/\mu\|_F^2$ , we have  $\partial \mathcal{J}_2 / \partial X = \mu(X + E - M + Q/\mu)$ .  $\partial \mathcal{J}_1 / \partial X$  can be computed by the chain rule

$$\frac{\partial \mathcal{J}_1}{\partial X} = \sum_{i=1}^n \sum_{j=1}^n \frac{\partial \mathcal{J}_1}{\partial K_{ij}} \frac{\partial K_{ij}}{\partial X}, \quad (29)$$

where

$$\frac{\partial \mathcal{J}_1}{\partial K} = \frac{1}{2} K^{-\frac{1}{2}}. \quad (30)$$

The second step for minimizing  $\mathcal{L}(X, E, Q)$  is to fix  $X$  and solve

$$\min_E \lambda\|E\|_1 + \frac{\mu}{2}\|X + E - M + Q/\mu\|_F^2. \quad (31)$$

The closed-form solution of (31) is given as

$$E = \Theta_{\lambda/\mu}(M - X - Q/\mu), \quad (32)$$

where  $\Theta(\cdot)$  is the element-wise soft thresholding operator [26] defined as

$$\Theta_\tau(u) = \frac{u}{|u|} \max\{|u| - \tau, 0\}. \quad (33)$$

Finally, the matrix of Lagrangian multipliers is updated by

$$Q \leftarrow Q + \mu(X + E - M). \quad (34)$$

The optimization frame for RKPCA is summarized in Algorithm 1. The convergence condition is

$$\frac{\mathcal{L}^{(t-1)}(X, E, Q) - \mathcal{L}^{(t)}(X, E, Q)}{\mathcal{L}^{(t-1)}(X, E, Q)} < \varepsilon \quad (35)$$

where  $\varepsilon$  is a small number such as  $10^{-6}$ .

---

#### Algorithm 1 Solve RKPCA with ADMM

---

**Input:**  $M, k(\cdot, \cdot), \lambda, \mu, t_{max}$ .

- 1: **initialize:**  $X^{(0)} = M, E^{(0)} = 0, t = 0$ .
- 2: **repeat**
- 3:  $X^{(t+1)} = X^{(t)} - \eta \left( \frac{\partial \mathcal{J}_1}{\partial X^{(t)}} + \frac{\partial \mathcal{J}_2}{\partial X^{(t)}} \right)$
- 4:  $E^{(t+1)} = \Theta_{\lambda/\mu}(M - X^{(t+1)} - Q/\mu)$
- 5:  $Q \leftarrow Q + \mu(X^{(t+1)} + E^{(t+1)} - M)$
- 6:  $t = t + 1$
- 7: **until** converged or  $t = t_{max}$

**Output:**  $X = X^{(t)}, E = E^{(t)}$

---

In Algorithm 1, a large  $\eta$  will increase the convergence speed but may make (26) diverge. It is known that the subproblem (26) will converge when  $\eta < 1/L_{\mathcal{J}}$ , where  $L_{\mathcal{J}}$  is the Lipschitz constant of the gradient of  $\mathcal{J}$  in (27) [24], [25]. The reason is that the gradient descent is the solution of the  $L_{\mathcal{J}}$  quadratic approximation, which is strongly convex [23]. In kernel methods such as SVM, KPCA and Gaussian processes, RBF kernel usually outperforms polynomial kernel. Similarly, we find that in RKPCA, RBF kernel is more effective than polynomial kernel. Hence, in this study, we mainly focus on RBF kernel. As suggested in a lot of work of kernel methods, the parameter  $\sigma$  can be chosen around the average of pair-wise distance of all data points, i.e.,

$$\sigma = \frac{\beta}{n^2} \sum_{i=1}^n \sum_{j=1}^n \|x_i - x_j\|, \quad (36)$$

where  $\beta$  can be chosen from  $\{0.5, 1, 1.5, 2\}$ . With RBF kernel, the gradient  $\partial \mathcal{J}_1 / \partial X$  can be computed as

$$\frac{\partial \mathcal{J}_1}{\partial X} = \frac{2}{\sigma^2} (XH - X \odot (BH)), \quad (37)$$

where  $H = \frac{\partial \mathcal{J}_1}{\partial K} \odot K = \frac{1}{2} K^{-1/2} \odot K$ ,  $B$  is a  $d \times n$  matrix of 1, and  $\odot$  denotes the Hadamard product. As can be seen, it is very difficult to obtain an available Lipschitz constant of the gradient because of the presence of kernel matrix. However, we can use inexact line search to find a good step size  $\eta$  that meets the sufficient decrease condition (Armijo-Goldstein inequality)

$$\mathcal{J}(X - \eta \frac{\partial \mathcal{J}}{\partial X}) < \mathcal{J}(X) - \gamma \eta \|\frac{\partial \mathcal{J}}{\partial X}\|_F^2, \quad (38)$$

where  $0 < \gamma < 1$ . The procedures of backtracking line search for  $\eta$  are shown in Algorithm 2. With the obtained  $\eta$ , the step 3 in Algorithm 1 will be non-expansive and the augmented Lagrangian function will decrease sufficiently. The optimization of RKPCA is in the nonconvex framework of ADMM studied in [24]. Therefore, the convergence of Algorithm 1 can be proved according to the approach in [24]. For simplicity, the proof will not be detailed in this paper.

---

**Algorithm 2** Backtracking line search for  $\eta$ 


---

**Input:**  $\eta = \eta_0$ ,  $c$  (e.g., 0.5),  $\gamma$  (e.g., 0.1).

- 1: **while**  $\mathcal{J}(X - \eta \frac{\partial \mathcal{J}}{\partial X}) > \mathcal{J}(X) - \gamma \eta \|\frac{\partial \mathcal{J}}{\partial X}\|_F^2$  **do**
- 2:    $\eta = c\eta$
- 3: **end while**

**Output:**  $\eta$

---

In Algorithm 2, we need to initialize  $\eta$  before hand. A large  $\eta_0$  may provide a broad search region to obtain a better solution but will need more iterations. We can compute a coarse estimation of  $L_{\mathcal{J}}$  to initialize  $\eta$  as

$$\eta_0 = 10/L_{\mathcal{J}}, \quad (39)$$

where

$$L_{\mathcal{J}} = \left\| \frac{2}{\sigma^2} (H - \rho) + \mu I \right\|_2. \quad (40)$$

In (40),  $I$  is an  $n \times n$  identity matrix and  $\|\cdot\|$  denotes the spectral norm of matrix. The estimation of  $L_{\mathcal{J}}$  is from  $\partial \mathcal{J} / \partial X$ , in which we have regarded  $H$  as a constant matrix not involved with  $X$  and replaced  $X \odot (BH)$  with  $\rho X$ . The reason is that  $H$  is related with  $K$  and the scaling factor  $\sigma^2$  has made the impact of  $X$  quite small. In addition, the elements of each row of  $BH$  are the same and hence we replace  $\odot BH$  by a number  $\rho$ , which is the average of all elements of  $BH$ . The derivation of (40) is detailed as follows.

$$\begin{aligned} & \left\| \frac{\partial \mathcal{J}}{\partial X_a} - \frac{\partial \mathcal{J}}{\partial X_b} \right\|_F = \left\| \frac{2}{\sigma^2} (X_a H_a - X_a \odot (BH_a) \right. \\ & \quad \left. - X_b H_b + X_b \odot (BH_b)) + \mu (X_a - X_b) \right\|_F \\ & \approx \left\| \frac{2}{\sigma^2} (X_a H - X_a \odot (BH) \right. \\ & \quad \left. - X_b H + X_b \odot (BH)) + \mu (X_a - X_b) \right\|_F \\ & \approx \left\| \frac{2}{\sigma^2} (X_a H - \rho X_a - X_b H + \rho X_b) + \mu (X_a - X_b) \right\|_F \\ & = \left\| (X_a - X_b) \left( \frac{2}{\sigma^2} (H - \rho) + \mu I \right) \right\|_F \\ & \leq \|X_a - X_b\|_F \left\| \left( \frac{2}{\sigma^2} H - \rho \right) + \mu I \right\|_2 \end{aligned} \quad (41)$$

Therefore,  $\alpha L_{\mathcal{J}}$  ( $0 < \alpha < 1$ ) could be an estimation of the Lipschitz constant of  $\frac{\partial \mathcal{J}}{\partial X}$  if  $\alpha$  is small enough. We found that when  $\eta_0 = 10/L_{\mathcal{J}}$ , Algorithm 2 can find  $\eta$  in at most 5 iterations.

In [24], it was shown that ADMM is able to converge to the set of stationary solutions, provided that the penalty parameter in the augmented Lagrangian is large enough and all the subproblems do not diverge, although the objective function is nonconvex. Therefore, in RKPCA, if the step size  $\eta$

is small enough and the Lagrangian penalty  $\mu$  is large enough, Algorithm 1 will converge to a stationary solution. Similar to the optimization of RPCA and other methods solved by ADMM, the Lagrangian penalty  $\mu$  in Algorithm 1 is quite easy to determine. We can just set  $\mu = 10\lambda$ . In fact, ADMM is not sensitive to the Lagrangian penalty.

2) *Proximal linearized minimization with adaptive step size (PLM+AdSS):* In RKPCA, problem (18) can be rewritten as

$$\min_E \text{tr}(K^{1/2}) + \lambda \|E\|_1, \quad (42)$$

where  $K$  is the kernel matrix carried out on  $M - E$ . We denote the objective function of (42) by  $\mathcal{J}$ . RKPCA in the form of (42) has no constraint and has only one block of variables. Hence, we propose to solve (42) by proximal linearized minimization with adaptive step size (PLM+AdSS), which is shown in Algorithm 3. At  $t$ -th iteration, we linearize  $\text{tr}(K^{1/2})$  at  $E^{(t-1)}$  as

$$\begin{aligned} \text{tr}(K^{1/2}) = & \text{tr}(K_{t-1}^{1/2}) + \left\langle \frac{\partial \mathcal{J}}{\partial E^{(t-1)}}, E - E^{(t-1)} \right\rangle \\ & + \frac{\nu}{2} \|E - E^{(t-1)}\|_F^2, \end{aligned} \quad (43)$$

where  $\nu$  is the step size and

$$\frac{\partial \mathcal{J}}{\partial E^{(t-1)}} = -\frac{2}{\sigma^2} ((M - E^{(t-1)})H - (M - E^{(t-1)}) \odot (BH)). \quad (44)$$

Then we solve

$$\min_E \frac{\nu}{2} \|E - E^{(t-1)} + \frac{\partial \mathcal{J}}{\partial E^{(t-1)}}/\nu\|_F^2 + \lambda \|E\|_1, \quad (45)$$

for which the solution is

$$E^{(t)} = \Theta_{\lambda/\nu}(E^{(t-1)} - \frac{\partial \mathcal{J}}{\partial E^{(t-1)}}/\nu). \quad (46)$$

The Lipschitz constant of  $\frac{\partial \mathcal{J}}{\partial E^{(t-1)}}$  could be a good value of the step size  $\nu$ . Similar to (41), we can estimate the Lipschitz constant of  $\frac{\partial \mathcal{J}}{\partial E^{(t-1)}}$  as

$$\hat{L}_{\nabla \mathcal{J}} = \left\| \frac{2}{\sigma^2} H - \rho \right\|_2. \quad (47)$$

In Algorithm 3, we set  $\nu$  as  $\omega \hat{L}_{\nabla \mathcal{J}}$  and increase  $\omega$  by  $\omega = c\omega$  if the objective function does not decrease. The convergence condition of Algorithm 3 is  $\|E^{(t)} - E^{(t-1)}\|_F / \|M\|_F < \varepsilon$  (e.g.  $10^{-4}$ ). We have the following lemma:

**Lemma 2.** (a) The objective function in Algorithm 3 is able to converge to a local minima. (b) The solution of  $E$  generated by Algorithm 3 is able to converge if  $t$  is large enough.

The above lemma will be proved in the following content.

The problem of RKPCA given by (42) is a case of the following general problem

$$\min_v J(v) = f(v) + g(v), \quad (48)$$

where  $f(\cdot)$  is nonconvex but differentiable and  $g(\cdot)$  is convex but not differentiable. We linearize  $f(v)$  at  $\bar{v}$  as

$$f(v) = f(\bar{v}) + \langle v - \bar{v}, \nabla f(\bar{v}) \rangle + \frac{\tau}{2} \|v - \bar{v}\|^2 + e, \quad (49)$$

---

**Algorithm 3** Solve RKPCA with PLM+AdSS

---

**Input:**  $M, k(\cdot, \cdot), \lambda, \omega = 0.1, c > 1, t_{max}$ .

1: **initialize:**  $E^{(0)} = 0, t = 0$ 

2: **repeat**

3:   Compute  $\frac{\partial \mathcal{J}}{\partial E^{(t-1)}}$  by (44)

4:    $\nu = \omega \left\| \frac{2}{\sigma^2} H - \rho \right\|_2$ 

5:    $E^{(t)} = \Theta_{\lambda/\nu}(E^{(t-1)} - \frac{\partial \mathcal{J}}{\partial E^{(t-1)}}/\nu)$ 

6:   **if**  $\mathcal{J}(E^{(t)}) > \mathcal{J}(E^{(t-1)})$  **then**  $\omega = c\omega$ 

7:   **end if**

8:    $t = t + 1$ 

9: **until** converged or  $t = t_{max}$ 
**Output:**  $E = E^{(t)}, X = M - E$ 


---

where  $\nabla f(\bar{v})$  denotes the gradient of  $f(\cdot)$  at  $\bar{v}$  and  $e$  denotes the residual of the quadratic approximation. Then we solve

$$\min_v g(v) + \langle v - \bar{v}, \nabla f(\bar{v}) \rangle + \frac{\tau}{2} \|v - \bar{v}\|^2. \quad (50)$$

The closed-form solution is obtained by the proximal algorithm [26], i.e.,

$$v^+ \in \text{prox}_\tau^g(v - \nabla f(\bar{v})/\tau). \quad (51)$$

We give the following two lemmas.

**Lemma 3.** *If  $f(\cdot)$  is continuously differentiable and its gradient  $\nabla f$  is  $L_{\nabla f}$ -Lipschitz continuous, then*

$$f(v) \leq f(\bar{v}) + \langle v - \bar{v}, \nabla f(\bar{v}) \rangle + \frac{L_{\nabla f}}{2} \|v - \bar{v}\|^2. \quad (52)$$

**Lemma 4.** *Given that the gradient of  $f(\cdot)$  is  $L_{\nabla f}$ -Lipschitz continuous,  $v^+ \in \text{prox}_\tau^g(v - \nabla f(\bar{v})/\tau)$ , and  $\tau > L_{\nabla f}$ , we have*

$$f(v^+) + g(v^+) \leq f(\bar{v}) + g(\bar{v}) - \frac{\tau - L_{\nabla f}}{2} \|v^+ - v\|^2. \quad (53)$$

*Proof.* As  $v^+ \in \min_v g(v) + \langle v - \bar{v}, \nabla f(\bar{v}) \rangle + \frac{\tau}{2} \|v - \bar{v}\|^2$ , by taking  $v = \bar{v}$ , we have

$$g(v^+) + \langle v^+ - \bar{v}, \nabla f(\bar{v}) \rangle + \frac{\tau}{2} \|v^+ - \bar{v}\|^2 \leq g(\bar{v}). \quad (54)$$

Using Lemma 3 with  $v = v^+$ , we have

$$f(v^+) \leq f(\bar{v}) + \langle v^+ - \bar{v}, \nabla f(\bar{v}) \rangle + \frac{L_{\nabla f}}{2} \|v^+ - \bar{v}\|^2. \quad (55)$$

Adding (55) with (54), we have

$$f(v^+) + g(v^+) \leq f(\bar{v}) + g(\bar{v}) - \frac{\tau - L_{\nabla f}}{2} \|v^+ - v\|^2. \quad (56)$$

This finished the proof of Lemma 4.  $\square$

Lemma 4 shows that when  $\tau > L_{\nabla f}$ ,

$$J(v^{(t+1)}) < J(v^{(t)}) < \dots < J(v^{(1)}) < J(v^{(0)}). \quad (57)$$

where  $v^{(1)}, \dots, v^{(t+1)}$  is a series of  $v$  obtained from the proximal linearized algorithm. Since  $J(v) > -\infty$ , the proximal linearized algorithm is able to converge.

In Algorithm 3,  $\tau$  is estimated as  $\nu = \omega \hat{L}_{\nabla \mathcal{J}} = \omega \|2H/\sigma^2 - \rho\|_2$ . Let  $L_{\nabla \mathcal{J}}^{(t)}$  be the true Lipschitz constant of  $\frac{\partial \mathcal{J}}{\partial E^{(t)}}$  at  $t$ -th iteration. Let  $\nu^{(t)}$  be the estimated  $\tau$  at  $t$ -th iteration. We have

$$\mathcal{J}(E^{(t)}) - \mathcal{J}(E^{(t-1)}) \leq -\frac{\nu^{(t)} - L_{\nabla \mathcal{J}}^{(t)}}{2} \|E^{(t)} - E^{(t-1)}\|_F^2. \quad (58)$$

We increase  $\omega$  by  $\omega = c\omega$  if  $\mathcal{J}(E^{(t)}) - \mathcal{J}(E^{(t-1)}) > 0$ . If  $\omega^{(t)} > L_{\nabla \mathcal{J}}^{(t)}/\hat{L}_{\nabla \mathcal{J}}^{(t)}$ , we have  $\mathcal{J}(E^{(t)}) < \mathcal{J}(E^{(t-1)})$ . If  $c$  is large enough, there exists a number  $l > 1$  such that

$$\nu^{(t+1)} > L_{\nabla \mathcal{J}}^{(t+1)}, \nu^{(t+2)} > L_{\nabla \mathcal{J}}^{(t+2)}, \dots, \nu^{(t+l)} > L_{\nabla \mathcal{J}}^{(t+l)} \quad (59)$$

where  $\omega^{(t+l)} = \dots = \omega^{(t+1)} = \omega^{(t)}$ . Therefore,  $\mathcal{J}(E)$  will decrease with high probability even when  $\omega$  is relatively small. When  $\omega$  is large enough, we will always have  $\nu > L_{\nabla \mathcal{J}}$ . Since  $\mathcal{J}(E)$  is bounded, when  $t \rightarrow \infty$ ,  $\mathcal{J}(E^{(t)}) - \mathcal{J}(E^{(t)}) = 0$ . It means that the objective function in Algorithm 3 is able to converge. This proved Lemma 2(a).

Summing both sides of (58) from 1 to  $N$ , we have

$$\mathcal{J}(E^{(0)}) - \mathcal{J}(E^{(N)}) \geq \sum_{t=1}^N \frac{\nu^{(t)} - L_{\nabla \mathcal{J}}^{(t)}}{2} \|E^{(t)} - E^{(t-1)}\|_F^2, \quad (60)$$

which indicates that

$$\sum_{t=1}^{\infty} \frac{\nu^{(t)} - L_{\nabla \mathcal{J}}^{(t)}}{2} \|E^{(t)} - E^{(t-1)}\|_F^2 < \infty. \quad (61)$$

When  $t$  is small,  $\nu^{(t)} > L_{\nabla \mathcal{J}}^{(t)}$  holds with high probability. If  $t$  is larger than  $\bar{t}$  (when  $\omega$  reaches to a large enough value),  $\nu^{(t)} - L_{\nabla \mathcal{J}}^{(t)}$  always holds. Then we have

$$s + \sum_{t=\bar{t}}^{\infty} \frac{\nu^{(t)} - L_{\nabla \mathcal{J}}^{(t)}}{2} \|E^{(t)} - E^{(t-1)}\|_F^2 < \infty, \quad (62)$$

where  $s = \sum_{t=1}^{\bar{t}} \frac{\nu^{(t)} - L_{\nabla \mathcal{J}}^{(t)}}{2} \|E^{(t)} - E^{(t-1)}\|_F^2 \geq 0$ . It further indicates  $E^{(t)} - E^{(t-1)} = 0$  if  $t \rightarrow \infty$ . Therefore, the solution of  $E$  generated by Algorithm 3 is able to converge if  $t$  is large enough. This proved Lemma 2(b).

Compared with Algorithm 1, Algorithm 3 cannot ensure that the objective function is always decreasing when  $t$  is small. In Algorithm 2, to find a suitable  $\eta$ , it requires at least one iteration (for evaluating the objective function and gradient), which will increase the computational cost. These two algorithm will be compared in the section of experiments.

The main computational cost of RKPCA is from the computation of  $K^{1/2}$  and its gradient, which requires to perform SVD on an  $n \times n$  matrix. Therefore, the computational complexity of RKPCA is  $O(n^3)$ . In RPCA, the main computational cost is from the SVD on a  $d \times n$  matrix. Hence, the computational complexity of RPCA is  $O(\min(d^2 n, dn^2))$ . RKPCA could be faster than RPCA if  $d > n$ . For large-scale data (e.g.,  $n > 5000$ ), instead of full SVD, truncated SVD or randomized SVD [27] should be applied to RKPCA.

### C. Robust subspace clustering by RKPCA

Similar to RPCA, RKPCA can also be applied to subspace clustering, even when the data are heavily corrupted. Given a noisy data matrix  $M$ , we use RKPCA to recover the clean data matrix  $X$ . The truncated singular value decomposition of the matrix in the nonlinear feature space is given by

$$\Phi(X) \approx U_r S_r V_r^T, \quad (63)$$

where  $r$  is the latent dimensionality of the feature space. The subspaces of  $\Phi(X)$  can be segmented by using  $V_r$ . We propose Algorithm 4 to cluster  $\Phi(X)$  or  $X$  according to the subspace membership. Similar to that in LRR [16], [18], the parameter  $p$  is an even number (e.g. 4) to ensure the non-negativity and sparsity of the affinity matrix  $A$ .

#### Algorithm 4 Subspace clustering by RKPCA

**Input:**  $M \in \mathbb{R}^{d \times n}$ ,  $C$ ,  $r$ ,  $p$ .

- 1: Compute  $X$  and the corresponding  $K$  using Algorithm 1 or Algorithm 3
- 2: Perform eigenvalue decomposition  $K \approx V_r S_r V_r^T$
- 3:  $[V_r]_{i \cdot} = [V_r]_{i \cdot} / \| [V_r]_{i \cdot} \|$ ,  $i = 1, 2, \dots, n$
- 4:  $A_{ij} = [V_r V_r^T]_{ij}^p$ ,  $A_{ij} = 0$ ,  $i, j = 1, 2, \dots, n$
- 5: Perform spectral clustering on  $A$

**Output:**  $C$  clusters of  $X$  or  $M$

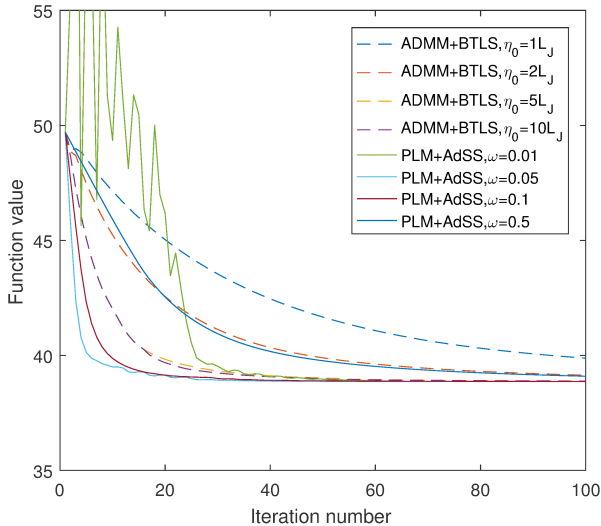


Fig. 1: Iteration performances of ADMM+BTLS and PLM+AdSS (for the first problem in Section III-A with 50% noise density)

## III. EXPERIMENTS

### A. Synthetic data

1) *Data generation:* We generate a nonlinear data matrix by

$$X = P_1 Z + 0.5(P_2 Z^{\odot 2} + P_3 Z^{\odot 3}) \quad (64)$$

where  $Z \in \mathbb{R}^{r \times n}$  are uniformly drawn from the interval  $(-1, 1)$ ,  $P \in \mathbb{R}^{d \times r}$  are drawn from standard normal distribution, and  $Z^{\odot u}$  denotes the  $u$ -th power acted on each entry of  $Z$ .

We set  $d = 20$ ,  $r = 2$ , and  $n = 100$ . The model (64) maps the low-dimensional latent variable  $z$  to high-dimensional variable  $x$  through a nonlinear function  $x = f(z)$ . The nonlinearity of the data is not very strong, which is quite practical because linearity and nonlinearity always exist simultaneously. We added Gaussian noises  $\mathcal{N}(0, 1)$  to certain percentage (noise density) of the entries in  $X$  and then get a matrix  $M$  with sparse noises. We increase the noise density from 10% to 70% and use PCA, KPCA [6], RPCA [11] and RKPCA to recover  $X$  from  $M$ . The recovery performance is measured by the relative error defined as

$$e_{rlt} = \|X - \hat{X}\|_F / \|X\|_F,$$

where  $\hat{X}$  denotes the recovered matrix. In KPCA and RKPCA, the parameter  $\sigma$  of RBF kernel is determined by (36) with  $\beta = 1$ .

2) *Iteration performances of ADMM+BTLS and PLM+AdSS:* Figure 1 shows the iteration performances of Algorithm 1 (ADMM+BTLS) and Algorithm 3 (PLM+AdSS) for solving RKPCA on the matrix with 50% noise density. It is found that, the two algorithms can work well with a large range of the parameters. In ADMM+BTLS,  $\eta = 10L_J$  and  $\eta = 5L_J$  achieve nearly the same results because the true Lipschitz constant may be around  $5L_J$ . In PLM+AdSS, though  $\omega = 0.01$  make the optimization diverged at the beginning of iteration, the algorithm still converged in about 60 iterations. In general, although ADMM+BTLS is able to reduce the objective function (augmented Lagrangian function) in every iteration, its convergence speed is lower than that of PLM+AdSS. In addition, the outputs of the two algorithms are nearly the same. Therefore, PLM+AdSS is preferable to ADMM+BTLS. In this paper, RKPCA is solved by PLM+AdSS with  $\omega = 0.1$ .

3) *Recovery results:* The experiments are repeated for 100 times and the average results are reported in Table I. As can be seen, the recovery error of RKPCA is significantly lower than those of other methods in almost all cases. We use (64) with  $d = 20$ ,  $r = 2$ , and  $n = 50$  to generate 5 matrices and stack them together to form a matrix of size  $20 \times 250$ . Hence the matrix consists of the nonlinear data drawn from 5 different subspaces. We add Gaussian noises  $\mathcal{N}(0, 1)$  to  $\delta$  (from 10% to 50%) percentage of the entries of the matrix. The recovery errors (average of 50 trials) are reported in Table II. RKPCA consistently outperforms other methods.

TABLE I: Relative errors (%) on single-subspace data

| $\delta$ | noisy | PCA   | KPCA  | RPCA        | RKPCA        |
|----------|-------|-------|-------|-------------|--------------|
| 10%      | 33.83 | 19.55 | 18.18 | <b>2.57</b> | 2.88         |
| 20%      | 49.59 | 26.63 | 25.73 | 10.56       | <b>5.03</b>  |
| 30%      | 63.07 | 32.36 | 33.01 | 19.06       | <b>11.21</b> |
| 40%      | 66.35 | 32.83 | 34.48 | 23.97       | <b>16.04</b> |
| 50%      | 81.95 | 40.02 | 41.69 | 32.54       | <b>26.18</b> |
| 60%      | 84.25 | 40.65 | 43.62 | 37.72       | <b>28.81</b> |
| 70%      | 93.74 | 45.26 | 47.85 | 44.38       | <b>36.92</b> |

### B. Natural images

1) *Datasets:* We use four datasets of natural images to evaluate the proposed method RKPCA. The details are as follows.

TABLE II: Relative errors (%) on multiple-subspace data

| $\delta$ | noisy | PCA   | KPCA  | RPCA  | RKPCA        |
|----------|-------|-------|-------|-------|--------------|
| 10%      | 35.22 | 31.84 | 25.82 | 26.27 | <b>10.08</b> |
| 20%      | 49.86 | 42.84 | 35.52 | 36.75 | <b>20.1</b>  |
| 30%      | 60.97 | 50.39 | 42.41 | 44.86 | <b>31.07</b> |
| 40%      | 68.49 | 55.29 | 47.39 | 49.95 | <b>38.16</b> |
| 50%      | 75.35 | 58.62 | 51.89 | 56.81 | <b>46.62</b> |

- **MNIST** [28] The dataset consists of the handwritten digits 0 ~ 9. We use a subset consisting of 1000 images (100 images for each digit) and resize all images to  $20 \times 20$ .
- **ORL** [29] The datasets consists of the face images of 40 subjects. Each subject has 10 images with different poses and facial expressions. The original size of each image is  $112 \times 92$ . We resize the images to  $32 \times 28$ .
- **COIL20** [30] The datasets consists of the images of 20 objects. Each object has 72 images of different poses. We resize the images to  $32 \times 32$ .
- **YaleB+** [31] The Extended Yale face dataset B consists of the face images of 38 subjects. Each subject has about 64 images under various illumination conditions. We resize the images to  $32 \times 32$ .

For each of the four datasets, we consider two noisy cases. In the first case (pixel-noisy), we add salt and pepper noise of 30% density to all the images. In the second case (block-noisy), we mask the images at random positions with a block of 20% width and height of the image. Since the backgrounds of the MNIST and COIL20 images are black, the value of the block mask is 1 while the value of the block mask for ORL and YaleB+ images is 0. Figure 2 shows a few examples of the original images and noisy images.

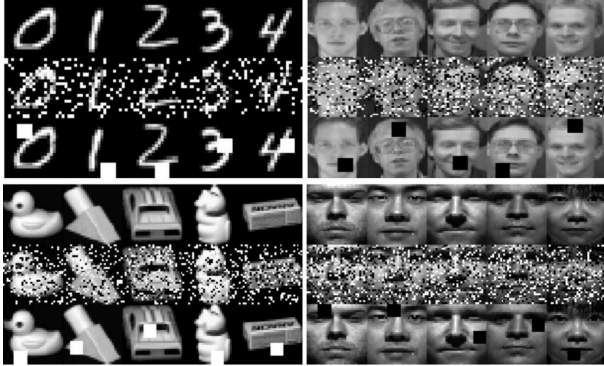


Fig. 2: A few samples of original images and noisy images (groups 1 ~ 4: MNIST, ORL, COIL20, YaleB+; in each group, rows 1 ~ 3: original, pixel-noisy, and block-noisy images)

2) *Noise removal*: We compare RKPCA with PCA, KPCA [6], and RPCA [11] in recovering the original images of the four datasets. The parameter  $\sigma$  of RBF kernel in KPCA and RKPCA is determined by (36) with  $\beta = 1.5$ . Since the original images especially that of MNIST and YaleB+ are noisy, we use one more evaluation metric, the generalization error of k-nearest neighbor, which is denoted by  $e_{knn}$ . A small value of  $e_{knn}$  indicates the intra-class difference is small compared to the inter-class difference. The average results of the relative

error and 5nn error of 10 repeated trials are reported in Table III. The relative recovery error and 5nn generalization error of RKPCA are always smaller than those of other methods. A few recovered images given by RPCA and RKPCA are shown in Figure 3. The recovery performances of RKPCA are consistently better than that of RPCA.

TABLE III: Relative recovery error (%) and 5nn generalization error (%) of noise removal on natural images

| Dataset | Case        | Metric    | PCA   | KPCA  | RPCA  | RKPCA        |
|---------|-------------|-----------|-------|-------|-------|--------------|
| MNIST   | pixel-noisy | $e_{rlt}$ | 75.8  | 69.27 | 53.61 | <b>48.13</b> |
|         |             | $e_{5nn}$ | 31.6  | 27.6  | 18.7  | <b>16.7</b>  |
|         | block-noisy | $e_{rlt}$ | 69.97 | 63.46 | 56.32 | <b>47.02</b> |
|         |             | $e_{5nn}$ | 39    | 38    | 24.3  | <b>19.9</b>  |
| ORL     | pixel-noisy | $e_{rlt}$ | 32.06 | 29.39 | 13.85 | <b>12.93</b> |
|         |             | $e_{5nn}$ | 60.75 | 49.25 | 6.75  | <b>5.75</b>  |
|         | block-noisy | $e_{rlt}$ | 26.75 | 25.11 | 17.05 | <b>11.23</b> |
|         |             | $e_{5nn}$ | 42.00 | 39.50 | 15.50 | <b>8.25</b>  |
| COIL20  | pixel-noisy | $e_{rlt}$ | 45.73 | 39.04 | 16.57 | <b>15.78</b> |
|         |             | $e_{5nn}$ | 5.83  | 5.66  | 0.76  | <b>0.56</b>  |
|         | block-noisy | $e_{rlt}$ | 34.65 | 31.28 | 18.2  | <b>14.3</b>  |
|         |             | $e_{5nn}$ | 9.37  | 9.16  | 3.96  | <b>1.46</b>  |
| YaleB+  | pixel-noisy | $e_{rlt}$ | 66.52 | 58.91 | 18.36 | <b>15.31</b> |
|         |             | $e_{5nn}$ | 74.68 | 75.68 | 53.32 | <b>46.72</b> |
|         | block-noisy | $e_{rlt}$ | 25.41 | 22.91 | 18.04 | <b>13.96</b> |
|         |             | $e_{5nn}$ | 63.62 | 53.11 | 51.53 | <b>42.21</b> |

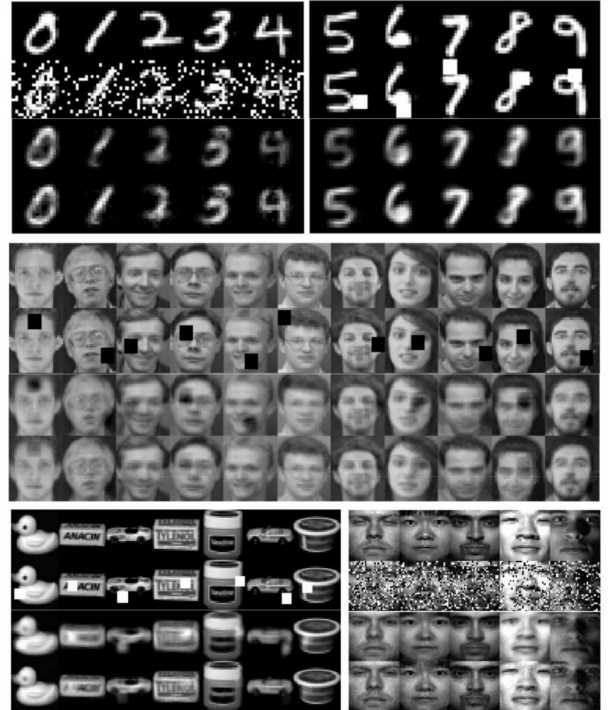


Fig. 3: Images recovered by RPCA and RKPCA (in each group, rows 1 ~ 4 are original, noisy, RPCA-recovered and RKPCA-recovered images)

3) *Subspace clustering*: We compare RKPCA with SSC [17], NLRR [18], RPCA [11] in subspace clustering on the four datasets. Particularly, we normalize all image vectors of YaleB+ dataset to have unit  $\ell_2$  norm because many images have very low brightness. The numbers ( $r$ ) of singular vectors for constructing the affinity matrices in NLRR, RPCA, and RKPCA on each dataset are as follows: MNIST,

$r_{NLRR} = r_{RPCA} = r_{RKPCA} = 50$ ; ORL,  $r_{NLRR} = r_{RPCA} = r_{RKPCA} = 41$ ; COIL20,  $r_{NLRR} = r_{RPCA} = 200$ ,  $r_{RKPCA} = 400$ ; YaleB+,  $r_{NLRR} = r_{RPCA} = r_{RKPCA} = 342$ . The parameters  $p$  (shown in Algorithm 4) for constructing the similarity graph in NLRR, RPCA, and RKPCA for the four datasets are set as  $p_{MNIST} = 8$ ,  $p_{ORL} = 4$ ,  $p_{COIL20} = 6$ , and  $p_{YaleB+} = 4$ . The clustering errors (averages of 10 repeated trials) are reported in Table IV. It is found that for the noisy images, SSC and NLRR have significantly higher clustering errors than RPCA and RKPCA do. The reason is that SSC and NLRR can not provide effective affinity matrices if the data are heavily corrupted. In contrast, RPCA and RKPCA are more robust to noises. RKPCA outperforms other methods significantly in all cases. Such clustering results are consistent with the previous noise removal results.

TABLE IV: Clustering errors (%) on natural images

| Dataset | Case        | SSC   | NLRR  | RPCA  | RKPCA        |
|---------|-------------|-------|-------|-------|--------------|
| MNIST   | original    | 35.2  | 29.4  | 30.7  | <b>26.2</b>  |
|         | pixel-noisy | 57.5  | 65.1  | 37.8  | <b>31.6</b>  |
|         | block-noisy | 70.1  | 62.6  | 50.4  | <b>37.3</b>  |
| ORL     | original    | 22.5  | 20.75 | 21.5  | <b>19.5</b>  |
|         | pixel-noisy | 25.75 | 36.5  | 22.75 | <b>19.5</b>  |
|         | block-noisy | 34.25 | 58.5  | 25.8  | <b>20.75</b> |
| COIL20  | original    | 14.29 | 17.92 | 16.72 | <b>13.26</b> |
|         | pixel-noisy | 32.06 | 36.58 | 21.82 | <b>15.42</b> |
|         | block-noisy | 31.86 | 39.04 | 26.34 | <b>18.61</b> |
| YaleB+  | original    | 22.26 | 17.46 | 18.25 | <b>13.63</b> |
|         | pixel-noisy | 65.1  | 73.02 | 28.5  | <b>26.17</b> |
|         | block-noisy | 40.87 | 35.12 | 27.92 | <b>24.41</b> |

#### IV. CONCLUSION

The proposed RKPCA solved the problem of high/full-rank matrix plus sparse noises, which is a challenge to existing methods such as RPCA. We proved the superiority of RKPCA over RPCA theoretically. RKPCA is so far the only unsupervised nonlinear method robust to sparse noises. We proposed two nonconvex algorithms, ADMM+BTLS and PLM+AdSS (with convergence proved), to solve the challenging optimization of RKPCA. PLM+AdSS is more efficient than ADMM+BTLS. Thorough comparative studies showed RKPCA significantly outperformed PCA, KPCA, RPCA, SSC and NLRR in noise removal or/and subspace clustering.

#### REFERENCES

- [1] I.T. Jolliffe. *Principal Component Analysis*. Springer Series in Statistics. Springer, 2002.
- [2] Bernhard Scholkopf, Alexander Smola, and Klaus-Robert Mller. Non-linear component analysis as a kernel eigenvalue problem. *Neural Computation*, 10(5):1299–1319, 1998.
- [3] Heiko Hoffmann. Kernel pca for novelty detection. *Pattern Recognition*, 40(3):863 – 874, 2007.
- [4] Jicong Fan, S. Joe Qin, and Youqing Wang. Online monitoring of nonlinear multivariate industrial processes using filtering kicapca. *Control Engineering Practice*, 22:205 – 216, 2014.
- [5] Sebastian Mika, Bernhard Schlkopf, Alex Smola, Klaus-Robert Mller, Matthias Scholz, and Gunnar Rtsch. Kernel pca and de-noising in feature spaces. In *Advances in Neural Information Processing Systems 11*, pages 536–542. MIT Press, 1999.
- [6] J. T. Y. Kwok and I. W. H. Tsang. The pre-image problem in kernel methods. *IEEE Transactions on Neural Networks*, 15(6):1517–1525, Nov 2004.
- [7] W. S. Zheng, J. Lai, and P. C. Yuen. Penalized preimage learning in kernel principal component analysis. *IEEE Transactions on Neural Networks*, 21(4):551–570, April 2010.
- [8] Minh H Nguyen and Fernando Torre. Robust kernel principal component analysis. In *Advances in Neural Information Processing Systems*, pages 1185–1192, 2009.
- [9] Lei Xu and Alan L Yuille. Robust principal component analysis by self-organizing rules based on statistical physics approach. *IEEE Transactions on Neural Networks*, 6(1):131–143, 1995.
- [10] Chris Ding, Ding Zhou, Xiaofeng He, and Hongyuan Zha. R1-pca: Rotational invariant l1-norm principal component analysis for robust subspace factorization. In *Proceedings of the 23rd International Conference on Machine Learning*, ICML '06, pages 281–288, New York, NY, USA, 2006. ACM.
- [11] Emmanuel J. Candès, Xiaodong Li, Yi Ma, and John Wright. Robust principal component analysis? *J. ACM*, 58(3):1–37, 2011.
- [12] Zhouchen Lin, Minming Chen, and Yi Ma. The augmented lagrange multiplier method for exact recovery of corrupted low-rank matrices. *arXiv:1009.5055v3 [math.OC]*, 2010.
- [13] Emmanuel J. Candès and Benjamin Recht. Exact matrix completion via convex optimization. *Foundations of Computational Mathematics*, 9(6):717–772, 2009.
- [14] Q. Liu, Z. Lai, Z. Zhou, F. Kuang, and Z. Jin. A truncated nuclear norm regularization method based on weighted residual error for matrix completion. *IEEE Transactions on Image Processing*, 25(1):316–330, Jan 2016.
- [15] Jicong Fan and Tommy W.S. Chow. Matrix completion by least-square, low-rank, and sparse self-representations. *Pattern Recognition*, 71:290 – 305, 2017.
- [16] G. Liu, Z. Lin, S. Yan, J. Sun, Y. Yu, and Y. Ma. Robust recovery of subspace structures by low-rank representation. *IEEE Transactions on Pattern Analysis and Machine Intelligence*, 35(1):171–184, 2013.
- [17] E. Elhamifar and R. Vidal. Sparse subspace clustering: Algorithm, theory, and applications. *IEEE Transactions on Pattern Analysis and Machine Intelligence*, 35(11):2765–2781, 2013.
- [18] Jie Shen and Ping Li. Learning structured low-rank representation via matrix factorization. In *Proceedings of the 19th International Conference on Artificial Intelligence and Statistics*, pages 500–509, 2016.
- [19] Jiashi Feng, Huan Xu, and Shuicheng Yan. Online robust pca via stochastic optimization. In *Advances in Neural Information Processing Systems*, pages 404–412, 2013.
- [20] Soren Hauberg, Aasa Feragen, and Michael J Black. Grassmann averages for scalable robust pca. In *Proceedings of the IEEE Conference on Computer Vision and Pattern Recognition*, pages 3810–3817, 2014.
- [21] Qian Zhao, Deyu Meng, Zongben Xu, Wangmeng Zuo, and Lei Zhang. Robust principal component analysis with complex noise. In *International Conference on Machine Learning*, pages 55–63, 2014.
- [22] Daniel Pimentel-Alarcón and Robert Nowak. Random consensus robust pca. In *Artificial Intelligence and Statistics*, pages 344–352, 2017.
- [23] Stephen Boyd, Neal Parikh, Eric Chu, Borja Peleato, and Jonathan Eckstein. Distributed optimization and statistical learning via the alternating direction method of multipliers. *Found. Trends Mach. Learn.*, 3(1):1–122, 2011.
- [24] Mingyi Hong, Zhi-Quan Luo, and Meisam Razaviyayn. Convergence analysis of alternating direction method of multipliers for a family of nonconvex problems. *SIAM Journal on Optimization*, 26(1):337–364, 2016.
- [25] Wei Deng and Wotao Yin. On the global and linear convergence of the generalized alternating direction method of multipliers. *Journal of Scientific Computing*, 66(3):889–916, Mar 2016.
- [26] Neal Parikh and Stephen Boyd. Proximal algorithms. *Found. Trends Optim.*, 1(3):127–239, January 2014.
- [27] N. Halko, P. G. Martinsson, and J. A. Tropp. Finding structure with randomness: Probabilistic algorithms for constructing approximate matrix decompositions. *SIAM Review*, 53(2):217–288, 2011.
- [28] Y. Lecun, L. Bottou, Y. Bengio, and P. Haffner. Gradient-based learning applied to document recognition. *Proceedings of the IEEE*, 86(11):2278–2324, Nov 1998.
- [29] F. S. Samaria and A. C. Harter. Parameterisation of a stochastic model for human face identification. In *Proceedings of 1994 IEEE Workshop on Applications of Computer Vision*, pages 138–142, Dec 1994.
- [30] S. A. Nene, S. K. Nayar, and H. Murase. Columbia object image library (coil-20). Report, Columbia University, 1996.
- [31] Lee Kuang-Chih, J. Ho, and D. J. Kriegman. Acquiring linear subspaces for face recognition under variable lighting. *IEEE Transactions on Pattern Analysis and Machine Intelligence*, 27(5):684–698, 2005.